

BVRI Photometric Observations, Light Curve Solutions and Orbital Period Analysis of BF Pav

Atila Poro¹, Mark G. Blackford², Fahri Alicavus^{3,4}, Fatemeh Davoudi¹, Edwin Budding⁵,
PegahSadat MirshafieKhozani¹, Eduardo Fernández-Lajús^{6,7}, Jabar Rahimi¹,
Behjat Zarei Jalalabadi¹, Farzaneh Ahangarani Farahani¹

¹The International Occultation Timing Association Middle East section, Iran, info@iota-me.com

²Variable Stars South (VSS), Congarinni Observatory, Congarinni, NSW, Australia 2447, Australia

³Çanakkale Onsekiz Mart University, Faculty of Arts and Sciences, Department of Physics, 17020, Çanakkale, Turkey

⁴Çanakkale Onsekiz Mart University, Astrophysics Research Center and Ulupınar Observatory, 17020, Çanakkale, Turkey

⁵Carter Observatory, 40 Salamanca Rd, Kelburn, Wellington 6012, New Zealand

⁶Instituto de Astrofísica de La Plata (CCT La Plata-CONICET-UNLP), La Plata, Argentina

⁷Facultad de Ciencias Astronómicas y Geofísicas, Universidad Nacional de La Plata, Paseo del Bosque, B1900FWA, La Plata, Argentina

Abstract

The new ephemeris and light curve analysis by synthesizing our mid-eclipse times and the former observations of BF Pav, that is classified as a W UMa-type eclipsing binary, are presented in this study. We also obtain this binary system's period changes using the Wilson-Devinney code after eight nights of observation in BVRI filters from two observatories in Australia and Argentina. Our results demonstrate that BF Pav is a contact binary system with a photometric mass ratio $q = 1.459 \pm 0.020$, a fillout factor $f = 9.9\%$, and an inclination of 89.31 ± 0.49 when in the light curve solutions we have a cold spot. We also calculated the distance of BF Pav $d = 240 \pm 21$ pc from the distance modulus formula, which is in good agreement with the distance obtained from this binary system's parallax in Gaia DR2. From our O-C analysis, we found a continuous period increase at a rate of 0.3079288×10^{-7} days/year which corresponds to a period increase of 0.266 s century⁻¹. We determined the mass of the primary component of this binary system using two different methods.

Key words: techniques: photometric — binaries: eclipsing — stars: individual (BF Pav)

1. INTRODUCTION

W UMa-type binary systems have short orbital periods less than a day showing continuous light variations (Dryomova and Svechnikov 2006). They include two stars usually surrounded by a common envelope resulting from mass overflowing one star's Roche lobe (Smith 1984).

The BF Pav binary system, which is located in the constellation of Pavonis in the Southern Hemisphere Sky, is a variable star of W UMa-type with an approximate period of 0.302318 days and G8 Spectral type (Gonzalez et al. 1996). Its apparent magnitude in V filter is 12.17 (APASS9). The variability of BF Pav was discovered by Shapley in 1939 (Gonzalez et al. 1996) and the first photoelectric light curve was obtained by Hoffman (1981). Although these observations did not cover the complete orbital period, the observer derived a period of 0.3056 days. Between 1987 and 1993, BF Pav was observed photoelectrically in the UBV filters in the observational program of Southern Short-Period Eclipsing Binaries to determine the times of minima, photometric and absolute parameters. The photometric solution adopted a mass ratio of $q = 1.4 \pm 0.2$, a fillout factor equals to 10%, and efficient thermal contact between the components, $\Delta T \sim 100$ K (Gonzalez et al. 1996).

Dryomova and Svechnikov (2006) found the rate of change of the period of BF Pav to be $\dot{p} = 1.62 \times 10^{-7}$ days/year in their study of variation in the orbital period of W UMa-type contact systems. Zhang et al. (2015) noted that BF Pav has a similar period increase to GK Aqr.

In this paper, we present a new ephemeris based on our observations as well as new period change analysis and light curve solutions.

2. OBSERVATION AND DATA REDUCTION

The observation of the BF Pav was carried out in September 2017, April 2018, August and June 2019, and July 2020 and a total of 3517 images were taken during eight nights. 2054 images were taken with a 14-inch Ritchey

Chretien telescope and SBIG STT3200-ME CCD equipped with Astroden Johnson-Cousins *BVR* Filters at the Congarinni Observatory which is located in Australia with geographical coordinates 152° 52' East and 30° 44' South and 20 meters above the mean sea level. Each frame was recorded at 2×2 binning with 50 seconds exposure time in each filter and CCD temperature set at -15°C. Also 1463 images were taken with a 2.15 m Jorge Sahade telescope and VersAreay 2048B CCD in V filter and each frame was recorded at 5×5 binning with 15 seconds exposure time at the Complejo Astronomico El Leoncito (CASLEO) Observatory located in Argentina with geographical coordinates 69° 18' West and 31° 48' South and 2 meters above the mean sea level.

GSC 8770-1511 was chosen as a check star and 8 stars were chosen as comparison stars with appropriate apparent magnitude in comparison to BF Pav. The general characteristics of BF Pav with the comparisons and the check star are shown in Table 1.

Table 1 Characteristic of the Variable star, the Check star, and the Comparison stars (from: SIMBAD¹ and Vizier-APASS9²).

Star type	Star name	RA. (2000)	DEC. (2000)	Magnitude (V)
Variable	BF Pav	18 45 39.32	-59 38 25.87	12.17
Comparison1	GSC 8770-1107	18 45 30.01	-59 32 34.9	12.23
Comparison2	GSC 8770-1582	18 45 50.08	-59 36 59.1	13.43
Comparison3	GSC 8770-1663	18 45 49.66	-59 37 48.9	13.43
Comparison4	GSC 8770-0085	18 45 33.39	-59 39 50.5	13.52
Comparison5	GSC 8770-103	18 46 0.36	-59 36 5.8	12.18
Comparison6	GSC 8770-1383	18 45 42.38	-59 32 5.3	13.39
Comparison7	GSC 8770-1325	18 45 18.25	-59 44 27.2	13.23
Comparison8	GSC 8770-1333	18 45 56.89	-59 40 26.6	13.54
Check	GSC 8770-1511	18 45 32.73	-59 36 25.0	13.48

Standard procedures for CCD image processing (aligned pictures, bias and dark removal, flat-fielding to correct for vignetting, and pixel-to-pixel variations) are applied. We did all picture processing and plotting raw images with MaxIm DL software. Then more modifications were made with AstrolmageJ (AIJ) software (Collins et al. 2017). AIJ is a powerful tool for astronomical image analysis and precise photometry (Davoudi et al. 2020). We determined 11 primary and 8 secondary minimum times from the observed light curves in *BVR* filters. These minima were calculated by using the Kwee and van Woerden (1956) method. The observed and synthetic light curves in *BVR* filters with residuals show in Figure 1.

¹<http://simbad.u-strasbg.fr/simbad/>

²<http://vizier.u-strasbg.fr/viz-bin/>

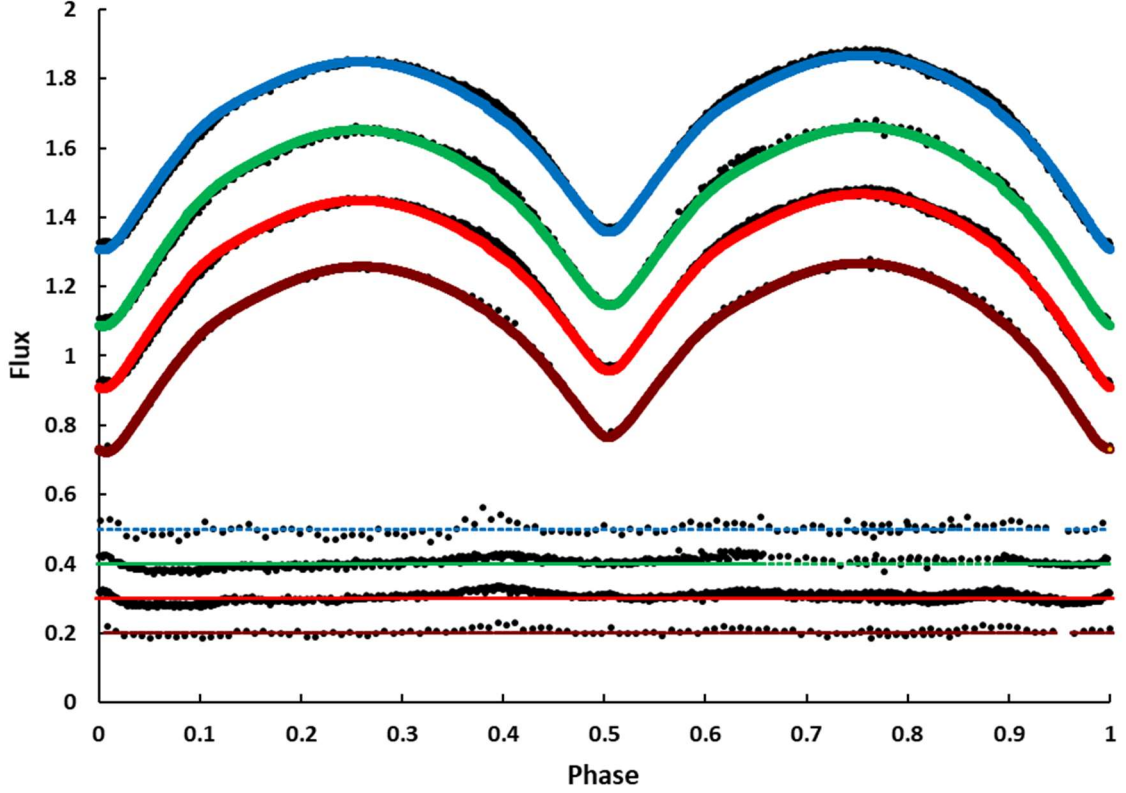


Fig.1 Observed light curves of BF Pav (points) and modeled solutions (lines) in the *BVRI* filter from top to bottom, respectively, and residuals are plotted; with respect to orbital phase, shifted arbitrarily in the relative flux.

3. ORBITAL PERIOD VARIATIONS

Using 50 mid-eclipse times including 26 primary and 24 secondary eclipses from the previous study and our observations, we analyze the orbital period variation of this system. All times of minimum listed in Table 2. It includes errors, method or filters of any observation, epochs, O-C values and the references of mid-eclipse times in the last column. We used the linear ephemeris of Gonzalez et al. (1996) for computing epochs and the O-C values.

$$\text{Min. 1 (BJD}_{\text{TDB}}) = 2448056.9013 (0.0002) + 0.30231864 (0.00000007) \times E \quad (1)$$

Table 2 Available times of minima for BF Pav.

BJD _{TDB}	Error	Method-Filter	Epoch	O-C	References
2444438.7617		Photoelectric	-11968	0.0099	GCVS 4 ³
2445886.4094	0.0001	Photometer	-7179.5	0.0048	IBVS 3265
2445886.5621	0.0003	Photometer	-7179	0.0063	IBVS 3265
2446936.8128		CCD	-3705	0.0021	PASP 108
2446936.8130		CCD	-3705	0.0023	PASP 108
2447259.8384		CCD	-2636.5	0.0002	PASP 108
2447259.8390		CCD	-2636.5	0.0008	PASP 108
2447259.8391		CCD	-2636.5	0.0009	PASP 108
2447368.6720		CCD	-2276.5	-0.0009	PASP 108
2447368.6721		CCD	-2276.5	-0.0008	PASP 108
2447368.6723		CCD	-2276.5	-0.0006	PASP 108
2448056.7487		CCD	-0.5	-0.0014	PASP 108

³<http://www.sai.msu.su/gcvs/gcvs/>

2448056.9008		CCD	0	-0.0005	PASP 108
2448056.9013	0.0002	CCD	0	0.0000	PASP 108
2448057.8074		CCD	3	-0.0009	PASP 108
2448057.8075		CCD	3	-0.0008	PASP 108
2448058.8656		CCD	6.5	-0.0008	PASP 108
2448058.8662		CCD	6.5	-0.0002	PASP 108
2449182.7358		CCD	3724	-0.0001	PASP 108
2449182.7361		CCD	3724	0.0002	PASP 108
2449184.7010		CCD	3730.5	0.0000	PASP 108
2449184.7007		CCD	3730.5	-0.0003	PASP 108
2449217.5030		CCD	3839	0.0004	PASP 108
2449217.5031		CCD	3839	0.0005	PASP 108
2449217.6545		CCD	3839.5	0.0008	PASP 108
2449217.6550		CCD	3839.5	0.0013	PASP 108
2449218.5619		CCD	3842.5	0.0012	PASP 108
2449218.5611		CCD	3842.5	0.0004	PASP 108
2449219.6189		CCD	3846	0.0001	PASP 108
2449219.6191		CCD	3846	0.0003	PASP 108
2457172.7180		CCD	30153	0.0027	OEJV 0179
2458015.5828	0.001	CCD-V	32941	0.0032	This study
2458227.8106	0.001	CCD-V	33643	0.0033	This study
2458639.7184	0.001	CCD-V	35005.5	0.0019	This study
2458639.8699	0.001	CCD-V	35006	0.0023	This study
2458701.9957	0.0001	CCD-R	35211.5	0.0016	This study
2458702.1472	0.0001	CCD-R	35212	0.0019	This study
2458710.9144	0.0001	CCD-R	35241	0.0019	This study
2458711.0653	0.0001	CCD-R	35241.5	0.0016	This study
2458713.9377	0.0001	CCD-R	35251	0.0020	This study
2458713.9377	0.0001	CCD-V	35251	0.0020	This study
2458713.9377	0.0001	CCD-I	35251	0.0020	This study
2458713.9380	0.0002	CCD-B	35251	0.0023	This study
2458714.0882	0.0001	CCD-I	35251.5	0.0014	This study
2458714.0883	0.0001	CCD-V	35251.5	0.0015	This study
2458714.0883	0.0002	CCD-B	35251.5	0.0015	This study
2458714.0884	0.0001	CCD-R	35251.5	0.0016	This study
2458716.9608	0.0001	CCD-V	35261	0.0019	This study
2458717.1116	0.0001	CCD-V	35261.5	0.0016	This study
2459060.9990	0.0004	CCD-R	36399	0.0015	This study

A new linear ephemeris was determined by fitting a line to mid-eclipse times using the least-squares method,

$$\text{Min. 1 (BJD}_{\text{TDB}}) = (2448056.90289 \pm 0.00217) + (0.30231864 \pm 0.00000006) \times E \text{ days} \quad (2)$$

where E is the cycle number after the reference cycle. Figure 2 shows the O-C diagram calculated using Equation 2. Where no error estimate was reported in the original references, we assumed a value equals to the largest reported error. The solid black line represents a quadratic least squares fit to the O-C values. The quadratic ephemeris is given in Equation 3,

$$\text{Min. 1 (BJD}_{\text{TDB}}) = (2448056.90198 \pm 0.00006) + (0.30231822 \pm 0.00000001) \times E + (1.274394 \pm 0.038495) \times 10^{-11} E^2 \text{ days.} \quad (3)$$

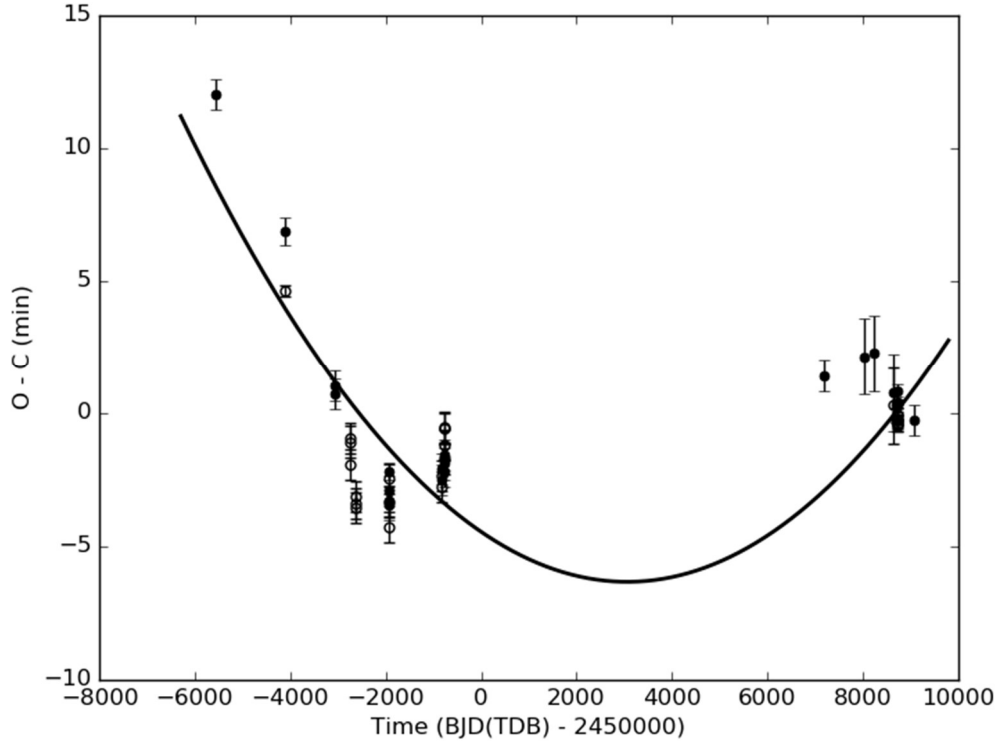


Fig. 2 The quadratic trend on the data points in residual of the linear fit.

We calculate \dot{p} , the rate of period change, using following formula according to a small quadratic term in the residue O-C,

$$\frac{dp}{dE} = 2Q \quad (4)$$

It reveals a continuous period increase at a rate of $0.3079288 \times 10^{-7} \text{ days/year}$ which corresponds to a period increase of $0.266 \text{ s century}^{-1}$.

The fitted quadratic trend in O-C was derived by the Monte Carlo Markov Chain (MCMC) approach in OCFit code⁴ with 1000000 MC steps and 20000 burn-in steps. Confidence interval plots for fitted parameters of p , t_0 , and Q ; and distributions of these parameters determined by the MCMC approach are displayed in Figure 3 and Figure 4, respectively.

⁴<https://github.com/pavolgaj/OCFit>

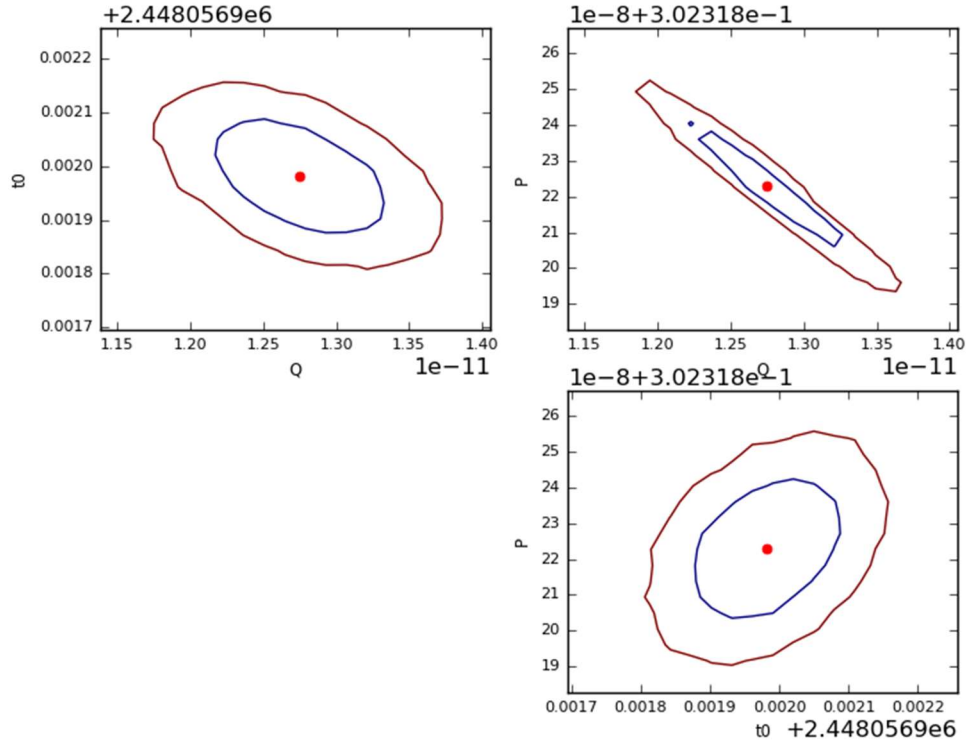


Fig. 3 The plot of Confidence Regions for $1\sigma=0.6827$ and $2\sigma=0.9545$ induced via the MCMC approach.

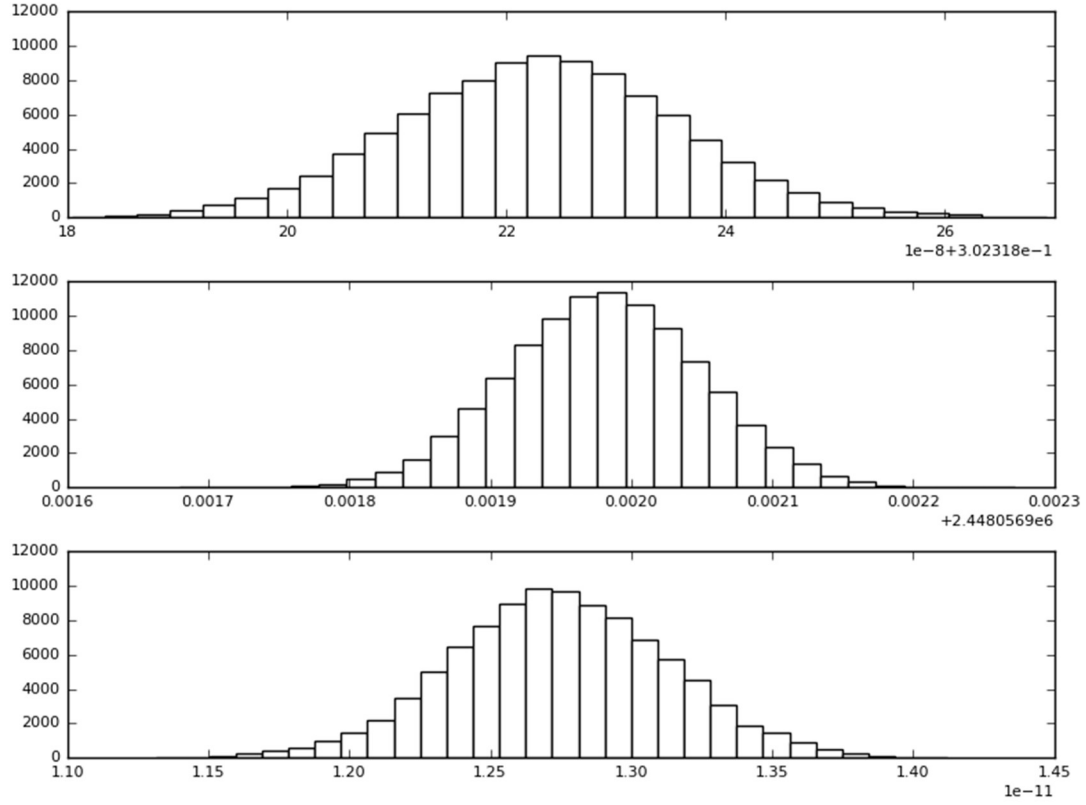


Fig. 4 Distribution of parameters of P , t_0 , and Q (from up to down respectively) induced by the MCMC approach.

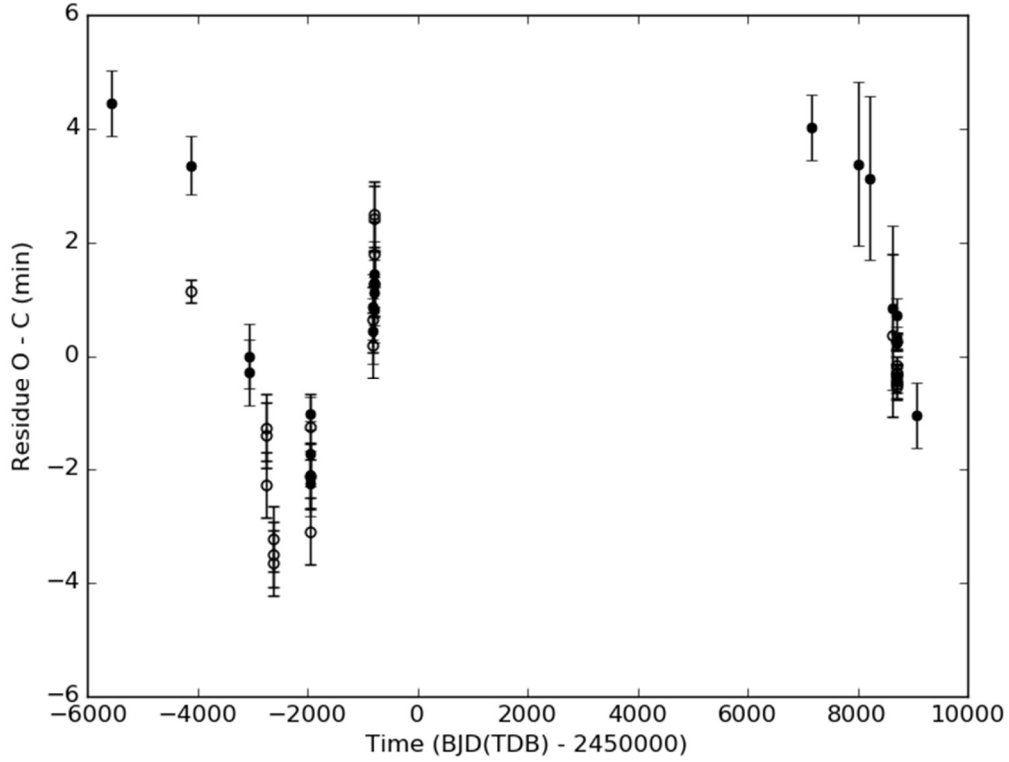


Fig. 5 A cyclic trend is seen in the residual of the quadratic trend of O-C.

In Figure 5, a cyclic change is seen in the residual of the quadratic term. It is maybe induced by the magnetic activity of components or Light-Time Effect (LiTE) that pointed to the presence of the additional body in the system. If we consider that this cyclic trend is due to the LiTE; a third body with a minimum mass ($M_3 \sin i$) ~ 0.1 MJ could be orbiting the binary, about 5 AU around the center of mass, and a period of ~ 6.4 yr.

4. LIGHT CURVE ANALYSIS

We used the Wilson-Devinney code (Wilson and Devinney 1971), to analyze the light curves. We have preferred to use the W-D code combined with the Monte Carlo simulation to determine the uncertainties of the adjustable parameters (Zola et al. 2004, 2010).

The mass ratio of the system could obtain by the q -search method in the photometric observations, so we did it according to the required standards (Rucinski 2005).

The $(B-V)$ color index is the difference in magnitudes between two wavelength filters B and V. The blue and visual magnitudes that they are measured through filters centered at 442 nm and 540 nm, respectively. Passing light through different filters depends on the star's surface temperature according to the Planck Law radiation distributions. It means that by having data of the Blue and Visual filters we can calculate the $(B-V)$ index and obtain a good estimation of a star's surface temperature by it (Poro et al. 2020).

The fraction of detected flux of wavelength depends on the telescope mirrors, the bandwidth of filters, and the response of the photometer, thus it is necessary to correct our data by calibration with the comparison stars from standard catalogs.

Many studies presented relations between the $(B-V)$ index and the surface temperature of the star such as Code et al. (1976), Sekiguchi and Fukugita (2000), and Ballesteros (2012). Eker et al. (2018) presented relations and tables for different parameters of the main-sequence stars. Eker et al. (2018) selected absolute parameters of 509 main-sequence stars from the components of detached-eclipsing spectroscopic binaries in the solar neighborhood that are used to study Mass-Luminosity, Mass-Radius, and Mass-Temperature relations. They combined the photometric data of Sejong Open cluster Survey (SOS) and typical absolute parameters adjusted from the MLR , MRR , and MTR functions calibrated in their study. 'Sejong Open cluster Survey (SOS) is a

photometry project of a large number of clusters in the SAAO Johnson-Cousins' *UBVI* system by Sung et al. (2013).

Based on our data and after calibrating (Høg et al. 2000), we calculated $(B-V)_{BF\ Pav} = 0^m.803$. As a result, based on Eker et al. (2018), the effective temperature of the primary component found to be 5201 K.

Sekiguchi and Fukugita (2000) derived a $(B-V)$ color-temperature relation too. They present T_{eff} as a function of $(B-V)$ color index to represent the metallicity value in four classes. By combining the previous results from Eker et al. (2018) and exerting the results of Sekiguchi and Fukugita (2000), the metallicity value for the primary component of BF Pav can be estimated between -0.75 and -0.25 (star's population II). As shown in Figure 6, obtained temperature from derived $(B-V)$ color is also in an acceptable range (4800 K - 5300 K) for the primary component of BF Pav with the method of Sekiguchi and Fukugita (2000).

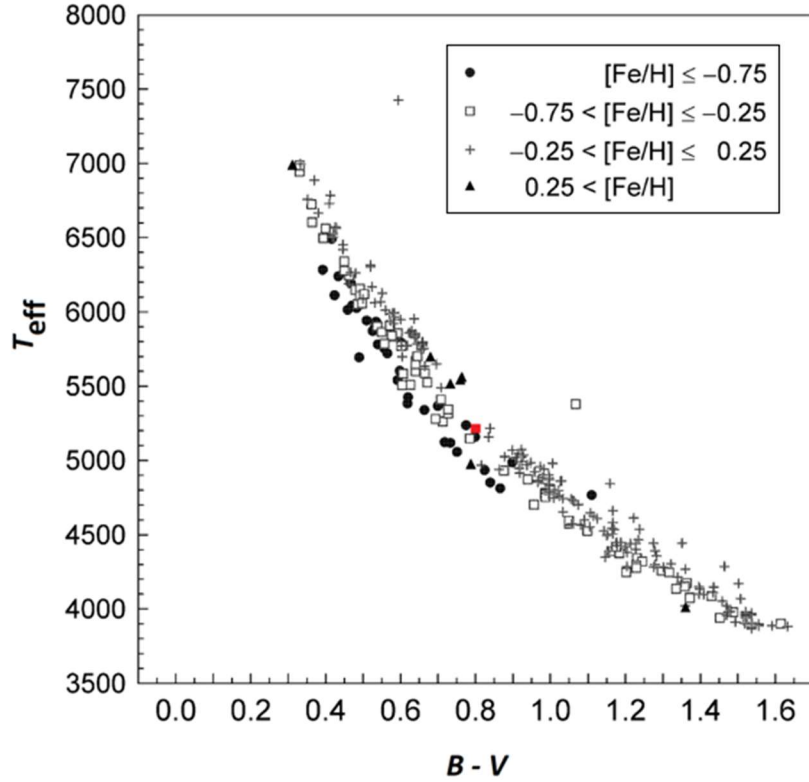


Fig. 6 BF Pav's position (red dot) based on the Sekiguchi and Fukugita (2000) results.

We assumed gravity-darkening coefficients $g_1 = g_2 = 0.32$ (Lucy 1967), bolometric albedo $A_1 = A_2 = 0.5$ (Rucinski 1969), and linear limb darkening coefficients taken from tables published by Van Hamme (1993).

As can be inferred from the light curves, the mean minimum occurred first, and also the temperature of the primary star is higher than the secondary. Based on the unequal minimums, and the logical light curve solutions, mode 3 was chosen for analysis. The parameters obtained from the solutions are given in Table 3. The mean fractional radii of components were calculated with the formula, $r_{mean} = (r_{back} \times r_{side} \times r_{pole})^{1/3}$ (5).

Table 3 Photometric solutions of BF Pav.

Parameter	Results (with a spot)	Results (without spot)
T_1 (K)	5201(13)	5201(13)
T_2 (K)	4980(20)	4944(19)
$\Omega_1=\Omega_2$	4.4073(297)	4.5438(193)
i (deg)	89.31(49)	89.62(46)
q	1.459(20)	1.561(13)
$I_1/I_{tot}(B)$	0.478(3)	0.474(2)

$l_2/l_{\text{tot}}(\text{B})$	0.522	0.526
$l_1/l_{\text{tot}}(\text{V})$	0.470(3)	0.465(2)
$l_2/l_{\text{tot}}(\text{V})$	0.530	0.535
$l_1/l_{\text{tot}}(\text{R})$	0.462(3)	0.456(2)
$l_2/l_{\text{tot}}(\text{R})$	0.538	0.544
$l_1/l_{\text{tot}}(\text{I})$	0.455(3)	0.447(2)
$l_2/l_{\text{tot}}(\text{I})$	0.545	0.553
$A_1 = A_2$	0.50	0.50
$g_1 = g_2$	0.32	0.32
f (%)	9.9	12.5
$r_1(\text{back})$	0.383	0.379
$r_1(\text{side})$	0.347	0.343
$r_1(\text{pole})$	0.331	0.327
$r_2(\text{back})$	0.449	0.457
$r_2(\text{side})$	0.417	0.425
$r_2(\text{pole})$	0.394	0.401
$r_1(\text{mean})$	0.354(2)	0.350(2)
$r_2(\text{mean})$	0.420(3)	0.428(2)
Colatitude _{spot} (deg)	28(6)	
Longitude _{spot} (deg)	0(1)	
Radius _{spot} (deg)	27(4)	
$T_{\text{spot}}/T_{\text{star}}$	0.80(2)	
$\sum(O - C)^2$	0.004	0.004
Phase Shift	0.001(1)	0.001(1)

Note: Parameters of a star spot is on the primary component.

Fillout factor is a quantity that indicates the degree of contact in the binary star systems defined by Mochnacki & Doughty (1972) and Lucy & Wilson (1979) that was modified and redefined by David H. Bradstreet (2005),

$$f = \frac{\Omega(L_1) - \Omega}{\Omega(L_1) - \Omega(L_2)} \quad (6)$$

where Ω , $\Omega(L_1)$, and $\Omega(L_2)$ are star surface potential, inner Lagrangian surface potential, and outer Lagrangian surface potential, respectively. We calculated a fillout factor of 9.9% with a cold spot and 12.5% without spot from the output parameters of the light curve solutions.

A difference in the heights of the maxima in light curves of eclipsing binary systems indicates the O'Connell effect (O'Connell 1951). This binary system appears to demonstrate this effect because we need to add a spot on the primary component in the light curve solutions. Table 4 represents the characteristic parameters of the light curves of BF Pav.

Table 4 Characteristic parameters of the light curves in the *BVR* filters.

Part of LC.	<i>B</i>	<i>V</i>	<i>R</i>	<i>I</i>
MaxI - MaxII	0.032	0.005	0.027	0.011
MaxI - MinI	-1.052	-0.982	-0.920	-0.879
MaxI - MinII	-0.868	-0.820	-0.783	-0.780
MinI - MinII	0.184	0.162	0.137	0.099

The $M_{\text{(primary)}}$ is derived from a study by Eker et al. (2018), and $M_{\text{(secondary)}}$ is calculated by $q = \frac{M_2}{M_1}$. We also calculated the mass of each component of the binary system using the method of Harmanec (1988) who derived a simple approximation formula relating absolute parameters (mass, radius and luminosity) to the effective temperature of the components based on data analyzing. For this purpose, we used the following formula,

$$\log M/M_{\odot} = ((1.771141X - 21.46965)X + 88.05700)X - 121.6782 \quad (7)$$

where X is $\log(T_{\text{eff}})$. This formula is only defined in the range of $4.62 \geq \log(T_{\text{eff}}) \geq 3.71$ (Harmanec 1988). So we calculated M_1 as the mentioned range is valid for primary T_{eff} of BF Pav due to our photometric solution. The absolute parameters are given in the Table 5 and there is a high conformity between the results which were obtained by two methods.

Table 5 Estimated absolute parameters of BF Pav by two methods to calculate the mass of the primary component.

Parameter	Eker et al. (2018)		Harmanec (1988)	
	Primary	Secondary	Primary	Secondary
Mass (M_{\odot})	0.914	1.333(21)	0.906(18)	1.322(18)
Radius (R_{\odot})	0.867(56)	1.061(53)	0.866(56)	1.059 (54)
Luminosity (L_{\odot})	0.493(72)	0.621(62)	0.492(61)	0.619(69)
M_{bol} (mag)	5.51(15)	5.26(15)	5.51(15)	5.26(15)
$\log g$ (cgs)	4.523(44)	4.511(42)	4.520(44)	4.510(42)
a (R_{\odot})	2.479(5)		2.475(5)	

According to the estimated absolute parameters of this binary system, the distance was calculated. We obtained $m_v = 12.674(25)$ from our light curve and $M_v = 5.691(30)$ for primary component ($BC_1 = -0.181$ from Eker et. al. 2018). So the distance to the binary system computed from the equation,

$$d_{(pc)} = 10^{\left(\frac{m_{pri} - M_{pri} + 5 - A_v}{5}\right)} \quad (8)$$

Therefore, an estimate of the distance of this binary system is 240 ± 21 parsec (using with $A_v = 0.08$ (Schlafly and Finkbeiner 2011)).

The 3D view of BF Pav and the Roche lobe configuration of BF Pav illustrated in Figure 7.

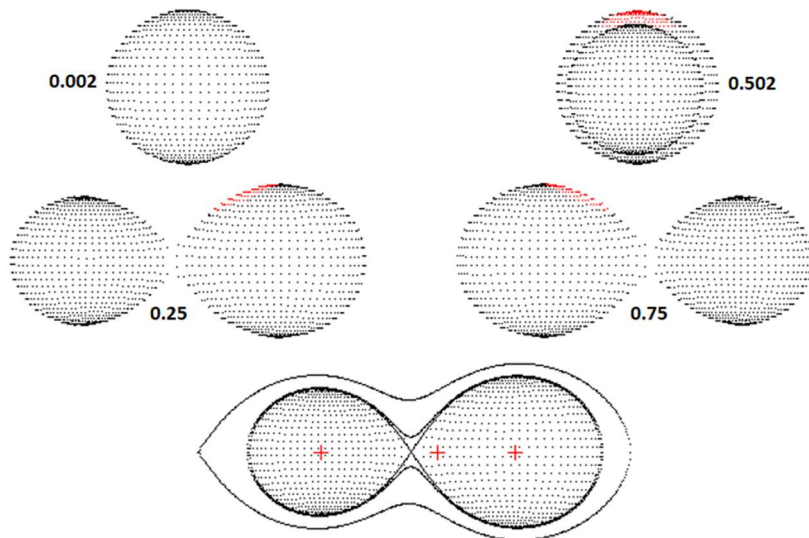


Fig. 7 The positions of the components of BF Pav.

5. RESULT AND CONCLUSION

This study's approach is to present a new ephemeris and light curve analysis of the W UMa-type eclipsing binary, BF Pav and probe this binary system's period changes. According to the O-C analysis, we obtain a period increase at a rate of 0.3079288×10^{-7} days/year.

The photometric observations of BF Pav were carried out during eight nights utilizing *BVR* filters from two observatories at Australia and Argentina. We specified the photometric solution of the short period system BF Pav based on the Wilson-Devinney code combined with the MC simulation to calculate the uncertainties of the searched parameters. Our results suggest that BF Pav is a contact binary with a mass ratio ($q = \frac{M_2}{M_1}$) of 1.459 ± 0.020 from q -search, a fillout factor (f) of 9.9%, and an inclination of 89.31 ± 0.49 . Also, the difference between this binary system components' temperature (ΔT) in the order of 200 K. Also, we calculated the binary system distance which is equal to 240 ± 21 pc and this result is in good agreement with the Gaia DR2⁵ value 255.084 ± 2.770 pc. We calculated the mass of the primary component of the binary system from two methods and their value were close to each other; then we calculated secondary mass by q value.

Based on the estimation of absolute parameters, the diagrams of the Mass-Luminosity (M - L) and the Mass-Radius (M - R) on a \log -scale (Figure 8) show the evolutionary status of BF Pav. The theoretical ZAMS and TAMS lines and the positions of the primary and secondary components are depicted in the diagrams.

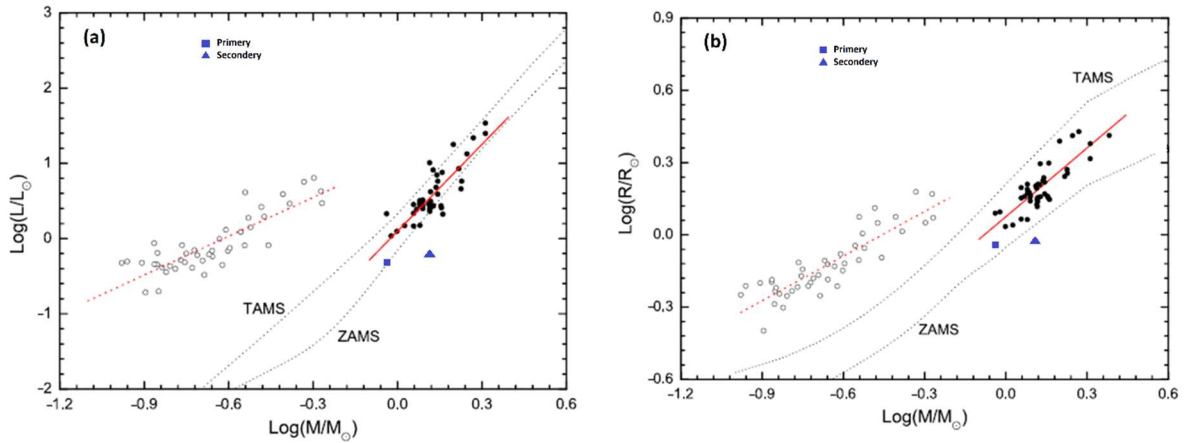


Fig. 8 The $\log M$ - $\log L$, and $\log M$ - $\log R$ diagrams for BF Pav from the absolute parameters.

Stellar winds are the major responsible for the binary system's mass loss due to the star's magnetic activities. According to the Table 4 and maxima differences in the light curves, it seems that BF Pav does not have significant magnetic activity and this implies a negligible O'Connell effect in this binary system, we fetched up that the mass loss idea is void for this system, so we concentrate on mass transfer. Based on the third Kepler law ($p^2 = \frac{4\pi^2}{G(M_1+M_2)} a^3$ (9)), by considering the angular momentum conservation law, we used the following formula (Negu and Tessema 2015):

$$\frac{\dot{p}}{p} = 3\dot{M}_1 \frac{(M_1 - M_2)}{M_1 M_2} \quad (10)$$

According to our results, the secondary star mass is more than primary star mass ($M_2 > M_1$) and also $\dot{p} > 0$ from our O-C analysis, so we derive that $\dot{M}_1 < 0$, thus the mass transfer is from the primary star to the

⁵<https://www.cosmos.esa.int/web/gaia/dr2>

secondary star, which causes $\dot{a} > 0$ ($\frac{\dot{p}}{p} = \frac{3}{2} \frac{\dot{a}}{a}$ (11)) that means the orbit enlarges and the angular frequency ($\frac{\dot{\omega}}{\omega} = \frac{-\dot{p}}{p}$ (12)) decreases.

BF Pav had been observed by Hoffman (1981) but the observer has not been able to prosecute a detailed analysis due to lack of data. After a while, the first detailed photometric analysis of BF Pav was performed in 1996 using the Wilson-Devinney code (Gonzalez et al. 1996) after *UBV* photoelectric observations of this binary system between 1987 and 1993 in the observational program of southern short-period eclipsing binaries. The former photometric solution demonstrates that BF Pav has a mass ratio of 1.4 while we calculated $q = 1.459 \pm 0.020$. To complete our comparison, we found 9.9% for the amount of fillout factor whereas 10% was obtained for f in the prior study. The temperature of the primary star reported 5430 K in the first photometric solution whereas we found 5201 K concerning the upper temperature limit value for this binary system's primary star is 5200 K in Gaia DR2. According to the amount of mass ratio, the fillout factor, and the inclination, which are in compliance with González et al (1996) results, we also suggest that BF Pav is a W-type system.

Since a cyclic change is seen in the residual of the quadratic term (Figure 5); it is maybe induced by the magnetic activity of components or LITE that pointed to the presence of the additional third body in the system. Therefore, BF Pav is a good choice for more photometric and spectroscopic observations in the future.

Acknowledgments This manuscript is based on the Binary Systems of South and North Project (<http://bsnp.info>). The project aims to study contact binary systems in the northern and southern hemispheres of several observatories in different countries.

References

- [1] Ballesteros, F.J., 2012. New insights into black bodies. *EPL (Europhysics Letters)*, 97(3), p.34008. <https://doi.org/10.1209/0295-5075/97/34008>.
- [2] Bradstreet, D.H., 2005, May. Fundamentals of solving eclipsing binary light curves using Binary Maker 3. In *Society for Astronomical Sciences Annual Symposium* (Vol. 24, p. 23).
- [3] Code, A.D., Bless, R.C., Davis, J. and Brown, R.H., 1976. Empirical effective temperatures and bolometric corrections for early-type stars. *The Astrophysical Journal*, 203, pp.417-434. <https://doi.org/10.1086/154093>.
- [4] Collins, K.A., Kielkopf, J.F., Stassun, K.G. and Hessman, F.V., 2017. AstrolmageJ: Image processing and photometric extraction for ultra-precise astronomical light curves. *The Astronomical Journal*, 153(2), p.77. <https://doi.org/10.3847/1538-3881/153/2/77>.
- [5] Davoudi, F., Jafarzadeh, S.J., Poro, A., Basturk, O., Mesforoush, S., Harandi, A.F., Gozarandi, M.J., Mehrjardi, Z.Z., Maley, P.D., Khakpash, S. and Rokni, K., 2020. Light curve analysis of ground-based data from exoplanets transit database. *New Astronomy*, 76, p.101305. <https://doi.org/10.1016/j.newast.2019.101305>.
- [6] Dryomova, G.N. and Svechnikov, M.A., 2006. Variation in the orbital period of W UMa-type contact systems. *Astrophysics*, 49(3), pp.358-369. <https://doi.org/10.1007/s10511-006-0036-9>.
- [7] Eker, Z., Bakış, V., Bilir, S., Soyduğan, F., Steer, I., Soyduğan, E., Bakış, H., Aliçavuş, F., Aslan, G. and Alpsoy, M., 2018. Interrelated main-sequence mass–luminosity, mass–radius, and mass–effective temperature relations. *Monthly Notices of the Royal Astronomical Society*, 479(4), pp.5491-5511. <https://doi.org/10.1093/mnras/sty1834>.
- [8] Gonzalez, J.F., Lapasset, E., Gomez, M. and Ahumada, J., 1996. Photometric Analysis of the Contact Binary BF Pavonis. *Publications of the Astronomical Society of the Pacific*, 108(722), p.338. <https://doi.org/10.1086/133727>.
- [9] Harmanec, P., 1988. Stellar masses and radii based on modern binary data. *Bulletin of the Astronomical Institutes of Czechoslovakia*, 39, pp.329-345.
- [10] Hoffmann, M., 1981. Photoelectric Photometry of BF Pavonis. *Information Bulletin on Variable Stars*, 1935.
- [11] Høg, E., Fabricius, C., Makarov, V.V., Bastian, U., Schwekendiek, P., Wicenec, A., Urban, S., Corbin, T. and Wycoff, G., 2000. Construction and verification of the Tycho-2 Catalogue. *Astronomy and Astrophysics*, 357, pp.367-386.

- [12] Juryšek, J., Hořková, K., Šmelcer, L., Mašek, M., Lehký, M., Bílek, F., Mazanec, J., Hanžl, D., Magris, M., Nosál, P. and Bragagnolo, U., 2017. BRNO Contributions# 40 Times of minima. *OEJV*, 179, p.1.
- [13] Kwee, K. and Van Woerden, H., 1956. A method for computing accurately the epoch of minimum of an eclipsing variable. *Bulletin of the Astronomical Institutes of the Netherlands*, 12, p.327.
- [14] Lucy, L.B., 1967. Gravity-darkening for stars with convective envelopes. *Zeitschrift fur Astrophysik*, 65, p.89.
- [15] Lucy, L.B. and Wilson, R.E., 1979. Observational tests of theories of contact binaries. *The Astrophysical Journal*, 231, pp.502-513. <https://doi.org/10.1086/157212>.
- [16] Mochnacki, S.W. and Doughty, N.A., 1972. A Model for the Totally Eclipsing W Ursae Majoris System AW UMa. *Monthly Notices of the Royal Astronomical Society*, 156(1), pp.51-65. <https://doi.org/10.1093/mnras/156.1.51>.
- [17] Negu, S.H. and Tessema, S.B., 2015. Mass Transfer in Binary Stellar Evolution and Its Stability. *International Journal of Astronomy and Astrophysics*, 5(03), p.222. <https://doi.org/10.4236/ijaa.2015.53026>.
- [18] O'Connell, D.J.K., 1951. The so-called periastron effect in eclipsing binaries. *Monthly Notices of the Royal Astronomical Society*, 111(6), pp.642-642. <https://doi.org/10.1093/mnras/111.6.642>.
- [19] Poro, A., Davoudi, F., Basturk, O., Esmer, E.M., Aksaker, N., Akyüz, A., Aladağ, Y., Rahimi, J., Lashgari, E., Ghanbarzadehchaleshtori, M. and Modarres, S., 2020. The First Light Curve Solutions and Period Study of BQ Ari. *arXiv preprint arXiv:2006.00528*.
- [20] Rucinski, S.M., 1969. The proximity effects in close binary systems. II. The bolometric reflection effect for stars with deep convective envelopes. *Acta Astronomica*, 19, p.245.
- [21] Rucinski, S.M., Pych, W., Ogłóza, W., DeBond, H., Thomson, J.R., Mochnacki, S.W., Capobianco, C.C., Conidis, G. and Rogoziecki, P., 2005. Radial velocity studies of close binary stars. X. *The Astronomical Journal*, 130(2), p.767. <https://doi.org/10.1086/431226>.
- [22] Schlafly, E.F. and Finkbeiner, D.P., 2011. Measuring reddening with Sloan Digital Sky Survey stellar spectra and recalibrating SFD. *The Astrophysical Journal*, 737(2), p.103. <https://doi.org/10.1088/0004-637X/737/2/103>.
- [23] Sekiguchi, M. and Fukugita, M., 2000. A Study of the B– V Color-Temperature Relation. *The Astronomical Journal*, 120(2), p.1072. <https://doi.org/10.1086/301490>.
- [24] Smith, R.C., 1984. The theory of contact binaries. *Quarterly Journal of the Royal Astronomical Society*, 25(4), pp.405-420.
- [25] Spencer Jones, J.H., 1988. The W UMa Stars AB Tel and BF Pav. *IBVS*, 3265, p.1.
- [26] Sung, H., Lim, B., Bessell, M.S., Kim, J.S., Hur, H., Chun, M.Y. and Park, B.G., 2013. Sejong open cluster survey (SOS). O. Target selection and data analysis. *arXiv preprint arXiv:1306.0309*. <https://doi.org/10.5303/JKAS.2013.46.3.103>.
- [27] Van Hamme, W., 1993. New limb-darkening coefficients for modeling binary star light curves. *The Astronomical Journal*, 106, pp.2096-2117. <https://doi.org/10.1086/116788>.
- [28] Wilson, R.E. and Devinney, E.J., 1971. Realization of accurate close-binary light curves: application to MR Cygni. *The Astrophysical Journal*, 166, p.605.
- [29] Zhang, L., Pi, Q., Han, X.L., Li, T., Zhang, X., Sang, H., Wang, D. and Wang, S., 2015. The first multi-color photometric study of the short-period contact eclipsing binary GK Aqr. *New Astronomy*, 38, pp.50-54. <https://doi.org/10.1016/j.newast.2015.02.002>.
- [30] Zola, S., Gazeas, K., Kreiner, J.M., Ogłóza, W., Siwak, M., Koziel-Wierzbowska, D. and Winiarski, M., 2010. Physical parameters of components in close binary systems—VII. *Monthly Notices of the Royal Astronomical Society*, 408(1), pp.464-474. <https://doi.org/10.1111/j.1365-2966.2010.17129.x>.
- [31] Zola, S., Rucinski, S.M., Baran, A., Ogłóza, W., Pych, W., Kreiner, J.M., Stachowski, G., Gazeas, K., Niarchos, P. and Siwak, M., 2004. Physical parameters of components in close binary systems: III. *Acta Astronomica*, 54, pp.299-312.